



HAL
open science

Towards Thermomechanical Heat Source Reconstruction in Presence of Advection Using Both Dic And Thermal Imaging

Jing Ye, Neveu Alain, Farge Laurent, Stephane Andre

► **To cite this version:**

Jing Ye, Neveu Alain, Farge Laurent, Stephane Andre. Towards Thermomechanical Heat Source Reconstruction in Presence of Advection Using Both Dic And Thermal Imaging. Photomechanics 2013, May 2013, Montpellier, France. 4p. hal-00920602

HAL Id: hal-00920602

<https://hal.science/hal-00920602>

Submitted on 19 Dec 2013

HAL is a multi-disciplinary open access archive for the deposit and dissemination of scientific research documents, whether they are published or not. The documents may come from teaching and research institutions in France or abroad, or from public or private research centers.

L'archive ouverte pluridisciplinaire **HAL**, est destinée au dépôt et à la diffusion de documents scientifiques de niveau recherche, publiés ou non, émanant des établissements d'enseignement et de recherche français ou étrangers, des laboratoires publics ou privés.

TOWARDS THERMOMECHANICAL HEAT SOURCE RECONSTRUCTION IN PRESENCE OF ADVECTION USING BOTH DIC AND THERMAL IMAGING

J. Ye, A. Neveu[†], L. Farge, S. André

Laboratoire d'Energétique et de Mécanique Théorique et Appliquée
UMR 7563 CNRS, Lorraine University
2, avenue de la Forêt de Haye,
BP160, 54504 Vandoeuvre-Lès-Nancy Cedex, France
jing.ye@univ-lorraine.fr, Laurent.Farge@univ-lorraine.fr, stephane.andre@univ-lorraine.fr

[†]Laboratoire de Mécanique et d'Energétique d'Evry
Université d'Evry Val d'Essonne
40 rue du Pelvoux CE1455, Courcouronnes, 91020 Evry Cedex, France
a.neveu@iut.univ-evry.fr

ABSTRACT: Thermomechanical investigation of solid materials using InfraRed imaging requires an inverse treatment of the temperature field to produce the intrinsic heat source field. Generally this is made assuming pure diffusion of heat which is valid in the regime of low Peclet numbers. In the case of plastic instabilities like the necking phenomenon observed when cold-drawing semi-crystalline polymers, the presence of non negligible advection is possible. which can produce a bias in the heat source reconstruction. It is then necessary to (i) measure precisely the velocity field during an experiment and (ii) use these data along with the measured temperature field to allows for a correct characterization of thermomechanical effects. We first discuss some experimental difficulties related to the measurement of velocity fields using DIC. A strategy is then presented that allows for heat source reconstruction in the diffusion-advection case.

1. INTRODUCTION

The difficult problem of measuring a source function of a Partial Differential Equation belongs to a fairly-well studied class of inverse problems. But the variety of differential operators used (variety of physical problems at stakes) as well as the variety of the looked objectives or of the available data sets make it still difficult to find a straightforward method with warranted results in all situations. In the field of thermomechanical applications, the data set is always obtained using InfraRed imaging and the heat source term has been reconstructed in many different ways but always from the pure diffusive heat equation [1, 2, 3]. For highly deformable materials like semi-crystalline polymers (HDPE) and high applied strain rates, quantifying the role of the advection phenomenon is necessary. We first present some experimental results of the heterogeneous velocity fields and relate the problems encountered to produce these data using DIC. In the second section, we present our first results regarding the inversion of transient temperature profiles when taking into account the convective transport of heat.

2. SOME EXPERIMENTAL CONSIDERATIONS REGARDING DIC VELOCITY FIELDS MEASUREMENTS

Digital Image Correlation (ARAMIS-3D system) is used to record pattern evolutions of markers on the surface of the specimen. The tensile test is controlled in real-time by video-extensometry to realize well-mastered experiments in terms of strain rates. InfraRed imaging is based on the use of a FLIR SC7000 camera. Both imaging systems are mounted on telescopic drives so that they can follow the central part of the specimen (approximately the same material point) during the test. This allows to follow the scene by keeping always the initial central material point in the center of the field of view of both cameras. This in turns, allows to reach high strain states, and to observe interesting evolutions of necking (central location onset and development of necking lips apart from it). The drawback is that the computation of displacements and strains cannot be obtained in a single step because of the very high deformation of the initial patterning. As a consequence, computations must be made in two steps with a new definition of patterns in between. This resets all displacement and strains but also re-defines a new set of material points (different from those used for the first stage). The difficulty is to append both data at a given resetting time and for truly identical material points. We get round this difficulty by identifying a typical material point in both stages. Figures (??) below shows the longitudinal strain computed for the two stages. It is clear that in the first stage, a material point exhibits a maximum strain which takes place in the center of the specimen. In the second stage, the strain is restarted to a 0 value and the evolution with time shows now two maximum strains obtained when the necking evolves along to propagating lips. It can be verified that for all acquisition time steps where the magnitude of both peaks is established, both the median point (perfect symmetry of the two peaks) nor the point with minimum strain value correspond to the same material point. These points remain very close one to each other (Fig.(2)). It is assumed that the material point with minimum value in the second stage corresponds to the material point having the strongest strain value in the first stage. With this matching condition, we can append both set of data. Additional treatment concerns the averaging of profiles in the transverse direction in order to reduce the Signal to Noise Ratio (SNR) which is important in

view of temporal numerical differentiation (centered stencil). Figure 4 illustrates the velocity profile that can be obtained from that treatment. Considering a typical length for thermal diffusion roughly equal to the distance between two facets used by DIC, this velocity profile obtained for a tensile test on HDPE at $\dot{\epsilon} = 1.2510^{-3}s^{-1}$ lead to maximum Peclet number of 0.05.

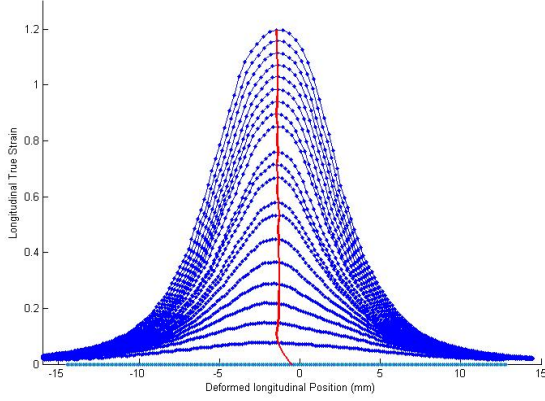


Figure 1 - $\dot{\epsilon}_y$ profile - Stage 1

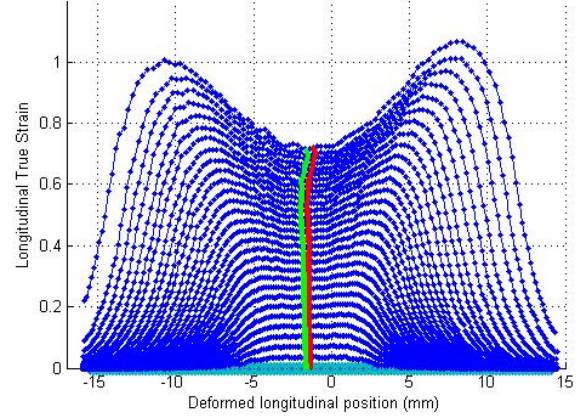


Figure 2 - $\dot{\epsilon}_y$ profile - Stage 2

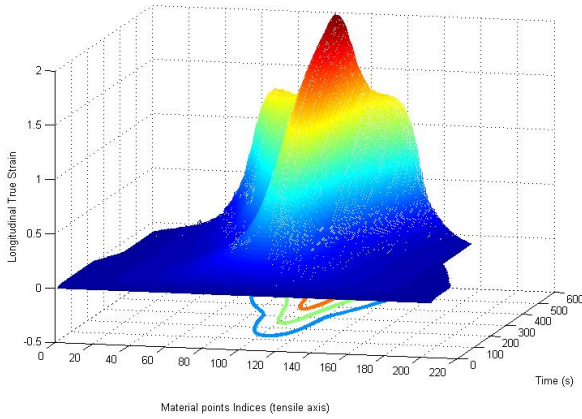


Figure 3 - $\dot{\epsilon}_y$ profile vs time for total experiment

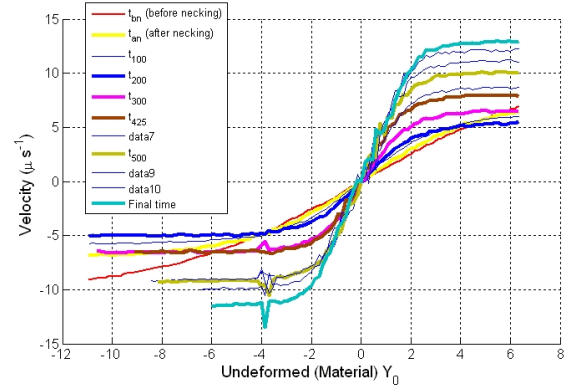


Figure 4 - Velocity Profile vs undeformed coordinate

3. INVERSE ALGORITHM

3.1 Test-case

The considered problem is given by the following equations (forward or direct model):

$$\begin{aligned} \forall x \in D = [0, L] \quad & c \frac{\partial T(x, t)}{\partial t} = k \frac{\partial^2 T(x, t)}{\partial x^2} - cv_0 \frac{\partial T(x, t)}{\partial x} + q(x) \quad \text{with } T(x, 0) = 0 \\ \forall t > 0 \quad & -k \frac{\partial T}{\partial x}(0, t) = -h_1 T \\ & -k \frac{\partial T}{\partial x}(L, t) = h_2 T \end{aligned} \quad (1)$$

This test case obtained from [4] departs from the real problem of our application in two things:

- the velocity field is considered uniform (v_0);
- the heat source term used as input is stationary $q(x)$ of C1-class (points of discontinuity are present).

To produce the synthetic data, we have considered the following values of the parameters (SI system): $c = 1, k = 0.03, h_1 = 0.1, h_2 = 0.02, t_{final} = 150s, v_0 = 0.1m/s$ and length $L = 1.5m$. The Peclet value is then equal to 5. The forward calculations are made either using FEM or FV techniques and uncorrelated random noise is added to the data before inversion tests.

3.2 Inversion method

It is based on a spectral method where regularization is performed separately on time and space as a result of the modal decomposition technique used for the temperature field $T(x, t) = \sum_{k=1}^N x_k(t) V_k(x)$. The modes $V_k(x)$ and the states $x_k(t)$ are obtained considering the Branch basis [5, 6] which main feature is to solve the so-called auxiliary problem (or eigenvalue problem) considering a generalized Steklov boundary condition. The corresponding set of equations has to be solve:

$$\begin{cases} \forall X \in D & k \frac{\partial^2 V}{\partial X^2} - cv_0 \frac{\partial V}{\partial X} = czV \\ -k \frac{\partial V}{\partial X} |_{X=0} = -(z\zeta + cv_0)V & -k \frac{\partial V}{\partial X} |_{X=L} = z\zeta V \end{cases} \quad (2)$$

where $\zeta = c * L/2$ is the Steklov number (arising naturally to preserve homogeneity of equations when eigenvalues z_k are considered both in the local balance equation and in the boundary conditions. For a non self-adjoint problem, the spectral branch basis is obtained when:

- a single "entering" advective flux is considered in the Steklov boundary equations
- Eigenmodes do form an orthogonal basis if adjoint eigenmodes are considered too (the output advective flux can now be considered)

The adjoint branch modes problem is given by

$$\begin{cases} \forall X \in D & k \frac{\partial^2 V^*}{\partial X^2} + cv_0 \frac{\partial V^*}{\partial X} = cz^* V^* \\ -k \frac{\partial V^*}{\partial X} |_{X=0} = -z^* \zeta V^* & -k \frac{\partial V^*}{\partial X} |_{X=L} = (z^* \zeta + cv_0) V^* \end{cases} \quad (3)$$

The set of functions (V_i, V_i^*) realizes a basis, respecting the bi-orthogonality condition:

$$\mathcal{E}_D(V_i, V_j^*) = \int_D c V_i \bar{V}_j^* dx + \zeta (V_i(b) \bar{V}_j^*(b) + V_i(a) \bar{V}_j^*(a)) = \delta_{i,j}$$

For this problem (2) and (3), eigen and adjoint modes can be computed analytically and the orthogonality condition can be easily checked numerically (of the order of 10^{-5}). Note that if v_0 is set equal to 0, one recovers the pure diffusive branch eigenmodes (which is a potential useful basis too).

If the decomposition $T(x, t) = \sum_{k=1}^N x_k(t) V_k(x)$ is now introduced in the original problem 1 and a variational weak formulation is applied, the following (classical) set of equations are obtained for the states:

$$\forall m \in 1, \dots, N \sum_{k=1}^N \dot{x}_k(t) \gamma_{km} = z_m x_m(t) - \sum_{k=1}^N x_k(t) Q_{km} - \sum_{k=1}^N x_k(t) P_{km} + \int_D q V_m dx \quad (4)$$

with

$$\gamma_{km} = \delta_{km} - \zeta \left(V_k(b) V_m^*(b) + V_k(a) V_m^*(a) \right)$$

$$Q_{km} = h_2 V_k(b) V_m^*(b) + h_1 V_k(a) V_m^*(a)$$

and

$$P_{km} = -cv_0 V_k(0) V_m^*(0)$$

The source term is decomposed on the same basis of branch functions according to $q(x, t) = \sum_{i=1}^{\infty} b_i(t) c V_i(x)$. A numerical system is obtained when considering the previously determined modes $V_k(x)$ and can be solved to calculate the states $x(t)$ of the temperature as a function of the coefficients $b_i(t)$ of the source [3]. In the presence of noise, regularization is obtained by truncating the decomposition to N_m modes and by applying the classical future time steps method [3].

3.3 Numerical inversion results

Figures 5,6 and 7 correspond to inversion results obtained at time $t = 0.5s$, Noise $\sigma = 1^\circ C$; $SNR \approx 15$, $N_m = 14$, $n_{tf} = 20$, $\sigma_{residuals} = 0.999$. Figure 6 shows the rebuild source from pure diffusive modes and figure 7 from advective-diffusive modes. In both cases, identification residuals for the temperature profile are identical and correspond to those plotted in fig. 5. The identification performs well even in this case of small Signal-to-Noise Ratio and is proved to be even better by using Diffusive eigenmodes instead of advective-diffusive modes for moderated Peclet number. This is of prime importance for practical applications.

4. PERSPECTIVES

Future developments of this work concerns the application of the inversion algorithm to cases of non-uniform velocity profiles (to understand the effect of a bias and noise on the velocity measurements to estimated heat source) and to the treatment of infrared images.

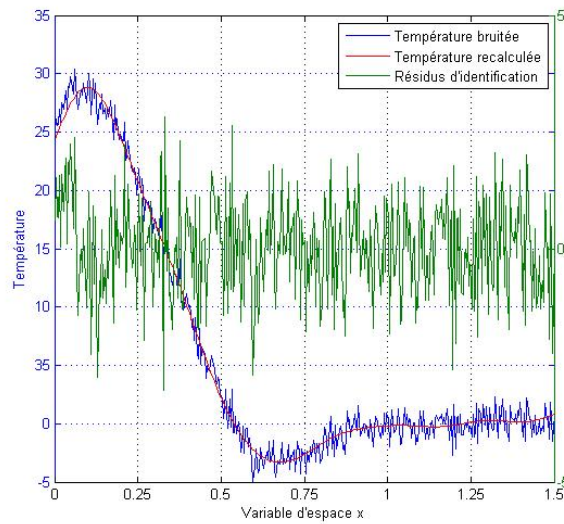


Figure 5 - Noisy synthetic temperature profile at $t = 0.5s$, rebuild profile and identification residuals

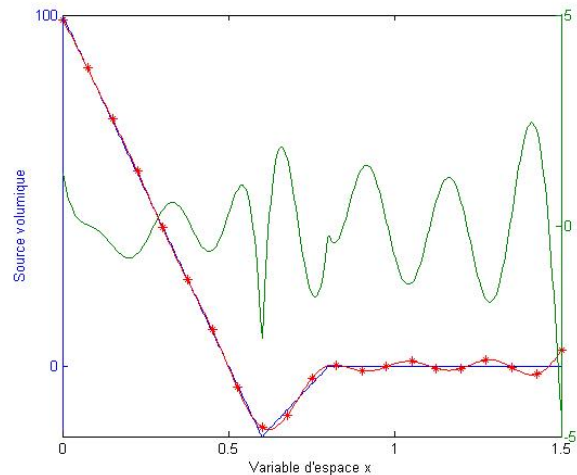
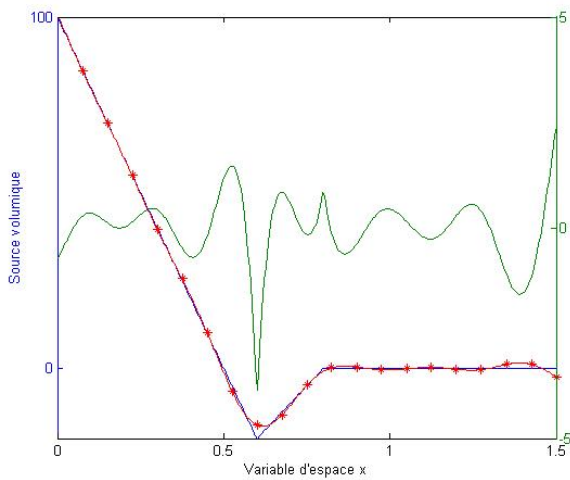


Figure 6 - Rebuild source with Diffusion Modes at $t = 0.5s$ Figure 7 - Rebuild source with Advection-Diffusion Modes at $t = 0.5s$

5. REFERENCES

1. Chrysochoos, A. and Louche, H. (2000) An infrared image processing to analyse the calorific effects accompanying strain localisation, *International Journal of Engineering Science* 38, 16, 1759-1788.
2. Doudard, CS., Calloch, S., Hild, F. and Roux, S. (2010) Identification of heat source from infrared thermography: Determination of 'self-heating' in a dual-phase steel by using a dog bone sample, *Mechanics of Materials* 42, 55-62.
3. Renault, N., Andre, S., Maillet, D. and Cunat, C. (2010) A spectral method for the estimation of a thermomechanical heat source from infrared temperature measurements, *International Journal of Thermal Sciences* 49, 8, 1394-1406.
4. Versteeg, H.K. and Malalasekera, W. (2007) Introduction to Computational Fluid Dynamics : The Finite Volume Method. *PEARSON Prentice Hall, 2nd ed.*
5. Quemener, O., Joly, F. and Neveu, A. (2010) On-line heat flux identification from a rotating disk at variable speed, *International Journal of Heat & Mass Transfer* 53, 7-8, 1529-1541.
6. Joly, F., Quemener, O., and Neveu, A. (2008) Modal reduction of an advection-diffusion model using a branch basis, *Numerical Heat Transfer, Part B* 53, 466-485.